UNIVERSITAT DE BARCELONA

A study of the shortwave schemes in the Weather Research and Forecasting model

Alex Montornès Torrecillas

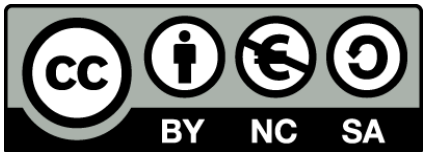

Chapter 2

From theory to parameterizations

Radiative transfer parameterizations in atmospheric models are necessary for two important reasons. On the one hand, the divergence of the flux in the vertical defines the heating and cooling rates in the atmosphere, a significant contribution in the diabatic term of the Euler equations (Montornès et al., 2015e). On the other hand, the surface fluxes have a significant impact on the surface energy balance parameterized within the Land Surface Model (LSM).

Although there are *exact* or high precision methods for solving the radiative transfer problem in planetary and stellar atmospheres, they can not be directly included in NWP models because i) they require high computational resources, unfeasible for an operative models and ii) the radiative variables are not prognosticated or diagnosed by the governing equations of the atmosphere and thus, they must be parameterized in terms of the thermodynamic fields (i.e. temperature, density, etc) and the outcomes of other physical schemes (e.g. microphysics).

The state–of–the–art related with the set of approximations used in NWP models is very extended. From text books that show a general overview with applications in modeling and remote sensing such as in Liou (1992), Lenoble (1993) or Liou (2002), among others, to more specific publications such as Stephens (1984) or Chou and Suarez (1999) that are directly focused on the radiative transfer parameterizations.

Nevertheless, without dealing with this matter exhaustively, we think that a brief chapter discussing the theoretical fundamentals of the approaches used by shortwave schemes can be useful as an introduction and for a better understanding of the following chapters. Particularly, Chapter 3 in which the solar parameterizations within the WRF-ARW model are analyzed.

The chapter starts from the beginning, with a presentation of the RTE in its general form (Sect. 2.1) and its general solution (Sect. 2.2). After this short introduction, we will present the approximated methods for solving the RTE implemented in NWP models (Sects. 2.3 and 2.4). Finally, Sect. 2.5 includes a description of the typical parameterizations used for evaluating the radiative transfer variables in terms of the meteorological fields provided by the NWP model, the main feature of each solar parameterization.

2.1 Radiative transfer equation

A beam emitted by the Sun travels through the vacuum for around 149.600.000 km until it reaches the Earth atmosphere. At this time, the atmospheric gases start absorbing one part of the incoming energy, decreasing the radiation that reaches the Earth surface. Due to the electronic distribution of each molecule, the different species in the atmosphere absorb energy at different parts of the solar spectrum. For example, ozone absorbs practically all energy contained in the ultraviolet region, being critical to protect the Deoxyribonucleic Acid (DNA) molecules and allowing the terrestrial life.

As it its explained in manuals such as Liou (1992), for a given wavelength λ, a pencil of solar radiation with a monochromatic intensity I_λ traveling through a medium with a thickness

ds and density ρ experiences an attenuation dI_λ (Fig. 2.1) that can be expressed as

$$dI_\lambda = -\rho k_\lambda I_\lambda ds, \tag{2.1}$$

where k_λ is the absorption coefficient, a physical property of the medium that represents the efficiency of that medium for absorbing radiation.

Concurrently, the solar beam is scattered by several elements such as gas molecules, aerosols, cloud water droplets, ice crystals, rain droplets or hail, among others. The light scattering in the visible region of the electromagnetic spectrum is something that we experience constantly. For example, when an incident beam reaches a surface, one part of the energy is scattered. This energy reaches our eyes making possible our vision of the world. In addition, gas molecules emit radiation that is overlapped with the scattering phenomena.

The scattered and emitted radiation by the medium (Fig. 2.2) increases the intensity with dI_λ that, formally, can be expressed as

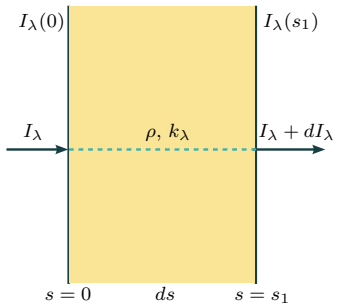

Figure 2.1: Radiative absorption of a layer represented by Eq. 2.1.

$$dI_\lambda = \rho j_\lambda ds, \tag{2.2}$$

where j_λ is called *Source function coefficient* and it has an analog role as k_λ but increasing the intensity.

Actually, absorption and scattering are physical processes that occur simultaneously. Mathematically, the combination of Eqs. 2.1 and 2.2 leads to

$$dI_\lambda = -\rho k_\lambda I_\lambda ds + \rho j_\lambda ds. \tag{2.3}$$

Eq. 2.3 can be simplified by defining a new magnitude called *Source function* as

$$J_\lambda = \frac{j_\lambda}{k_\lambda}. \tag{2.4}$$

With J_λ, we can rewrite Eq. 2.3 as

$$\frac{1}{k_\lambda \rho}\frac{dI_\lambda}{ds} = -I_\lambda + J_\lambda. \tag{2.5}$$

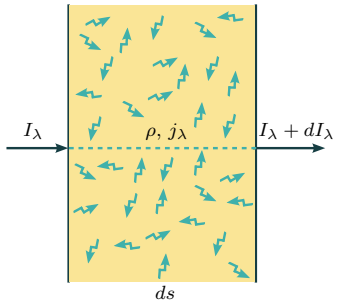

Figure 2.2: Radiative scattering represented by Eq. 2.2.

This equation is named RTE and it represents the most general expression for explaining the interaction between the radiation and matter (i.e. the atmosphere, a glass, etc).

The key to solve the RTE is in the evaluation of the source function J_λ that, generally, requires a complex treatment with successive approximations as will be explained in the next sections.

The most simple case is to consider a non-scattering medium. In this case, Eq. 2.5 becomes a simple differential equation expressed as

$$\frac{dI_\lambda}{k_\lambda \rho ds} = -I_\lambda. \tag{2.6}$$

Given a set of boundary conditions, the integration of Eq. 2.6 becomes trivial. If we assume that at $s = 0$, $I_\lambda = I_\lambda(0)$ and at $s = s_1$, $I_\lambda = I_\lambda(s_1)$, as shown in Fig 2.1, then the solution for Eq. 2.6 can be written as

$$I_\lambda(s_1) = I_\lambda(0) exp\left(-\int_0^{s_1} k_\lambda \rho ds\right). \tag{2.7}$$

As k_λ is a material property, it becomes a constant in a homogeneous medium and it can be replaced from the integral in Eq. 2.7. Moreover, by defining a new magnitude u named *path length*,

$$u = \int_0^{s_1} \rho ds, \tag{2.8}$$

Eq. 2.7 can be expressed as

$$I_\lambda(s_1) = I_\lambda(0) e^{-k_\lambda u}. \tag{2.9}$$

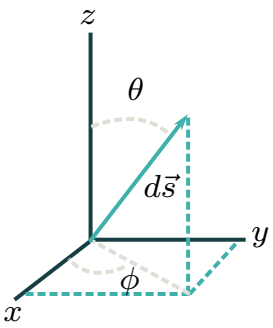

Figure 2.3: Solar beam in spherical coordinates.

This equation has different names as Beer's law, Lambert–Beer law, or the Beer–Lambert–Bouguer law. Note that Eq. 2.9 is independent of the beam direction and hence, it can be applied analogously to the flux computation and for this reason, it is an expression used in many radiative applications.

Based on Eq. 2.9, three new useful magnitudes can be introduced. In the first place, by dividing Eq 2.9 by $I_\lambda(0)$, we have a new variable T_λ describing the part of the radiation that travels through the medium without any scattering interaction. This variable is named *monochromatic transmissivity* or simply transmissivity and it can be written as

$$T_\lambda = \frac{I_\lambda(s_1)}{I_\lambda(0)} = e^{-k_\lambda u}. \tag{2.10}$$

The transmissivity ranges from 0 to 1 and it gives a quantification of how opaque is a medium. In the limit of $T_\lambda \to 0$, the medium is completely opaque in this wavelength while, for $T_\lambda \to 1$, the medium is transparent in this wavelength.

By the energy conservation principle, the radiation that is not transmitted, it is absorbed by the medium. Hence, we can define the *monochromatic absorptivity* A_λ as

$$A_\lambda = 1 - T_\lambda = 1 - e^{-k_\lambda u}. \tag{2.11}$$

Furthermore, in a scattering medium, Eq. 2.9 describes the attenuation of the monochromatic intensity in the direct direction from the emission source without considering the scattering interactions. Nevertheless, the radiation in these media is transmitted, absorbed but also reflected in all directions due to the scattering processes. The magnitude that quantifies this reflection is the *monochromatic reflectivity* R_λ. Hence, in a scattering medium the energy conservation principle becomes

$$A_\lambda + R_\lambda + T_\lambda = 1. \tag{2.12}$$

The determination of R_λ depends on the form of the source function, J_λ.

For most of the atmospheric applications, it is useful to assume that the atmosphere is composed by plane-parallel portions. Under this framework, the variation of the variables that describe the atmosphere (e.g. temperature, density or atmospheric composition) are only allowed in the vertical direction. Moreover, this approximation is natural in a NWP model because the simulation domain is composed by a set of vertical columns divided in

several vertical levels, each one representing the spatial averaged thermodynamic state of the meteorological fields.

Under the plane-parallel approximation, distances are convenient to be measured with respect to the normal of the stratification plane (Fig. 2.3). In other words, if z denotes the vertical distance and θ is the zenith angle of the emission source with respect to the normal, then, ds can be expressed as

$$ds = zcos\theta. \tag{2.13}$$

Besides, under the plane-parallel approximation, Eq. 2.5 can be expressed as

$$\mu \frac{dI_\lambda}{k_\lambda \rho dz} = -I_\lambda(z;\mu,\phi) + J_\lambda(z;\mu,\phi), \tag{2.14}$$

where $\mu = cos\theta$ and ϕ is the azimuth angle. When μ and ϕ are referred to the Sun's position, they are represented as μ_0 and ϕ_0, respectively.

Eq. 2.14 can be simplified by defining a new magnitude named *optical thickness* or depth τ_λ as

$$\tau_\lambda \equiv \int_z^\infty k_\lambda \rho dz', \tag{2.15}$$

measured downward from the TOA.

In a homogeneous medium, τ_λ is, trivially,

$$\tau_\lambda = k_\lambda u. \tag{2.16}$$

Finally, by substituting Eq. 2.15 into Eq. 2.14, we can write the RTE as

$$\mu \frac{dI_\lambda}{d\tau_\lambda} = -I_\lambda(\tau_\lambda,\mu,\phi) + J_\lambda(\tau_\lambda,\mu,\phi). \tag{2.17}$$

This is the general form of the RTE in a plane-parallel atmosphere, the point of departure for our discussion.

2.2 General solution of the RTE in the solar spectral region

In a scattering medium, the solution of the RTE (Eq. 2.17) depends on the form of the source function J_λ. As we aforementioned, J_λ describes the strengthening of the monochromatic intensity due to the molecular emission and the multiscattering processes, i.e.

$$J_\lambda = \text{EMISSION} + \text{SCATTERING}.$$

In Earth, the main emission source is found in the infrared (IR) region of the spectrum and it is produced by the atmospheric gases and Earth surface that can be approximated to a black body. As it is described in the literature, the source function of this emission can be expressed in terms of the Planck's function as

$$J_\lambda = B_\lambda(T). \tag{2.18}$$

This emission is modulated by an absorption coefficient $\beta_{a,\lambda}$ because the atmosphere absorbs partially this emission (i.e. greenhouse effect). Moreover, in virtue of the Kirchhoff law, absorption is equal to the emission and thus, we have

$$J_\lambda = \beta_{a,\lambda} B_\lambda(T). \tag{2.19}$$

However, in the Earth atmosphere the solar radiation (or shortwave) and the terrestrial radiation (or longwave) act in two well defined different spectral regions without practically overlapping (Fig. 2.4). Consequently, for most of the solar applications the emission in the IR region can be neglected. This consideration is useful for many of the atmospheric applications because it allows to solve the radiative transfer problem for shortwave and for longwave radiation, separately. In a NWP model, this approximation leads to two different parameterizations for representing the solar and the terrestrial radiative transfer processes.

In the shortwave spectral region, the radiative scattering can be considered as the sum of two contributions: i) the scattering of the direct beam emitted by the Sun and ii) the scattering of the diffuse radiation, called multiscattering. In both cases, it is necessary to know the angular distribution of the scattered light. In order to incorporate this information, we define a function named *phase function*, $P_\lambda(\cos\Theta)$, expressed in terms of the cosine of the scattering angle Θ which depends on the air molecules, cloud particles and aerosols. Trivially, in spherical coordinates (Fig. 2.3), the scattering angle can be written in terms of the input and output zenith and azimuth angles μ', ϕ' and μ, ϕ, respectively (Fig. 2.5).

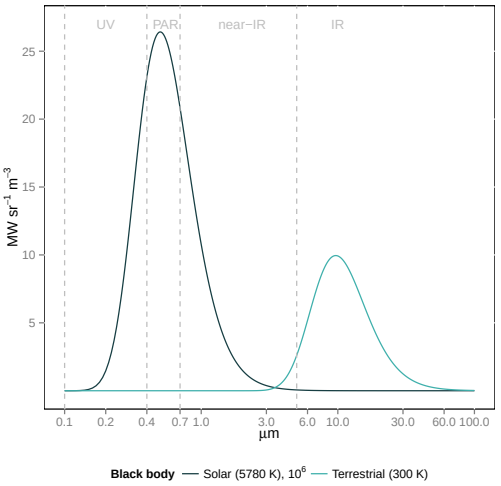

Figure 2.4: Solar and terrestrial black body spectral emission.

Under spherical geometry (e.g. plane-parallel approximation), the scattering angle can be written as

$$\cos\Theta = \mu\mu' + (1-\mu^2)^{1/2}(1-\mu'^2)^{1/2}\cos(\phi'-\phi). \tag{2.20}$$

Therefore, the scattering of the solar beam emitted by the Sun can be expressed in terms of the cosine of the solar zenith angle, μ_0 and a scattering coefficient $\beta_{s,\lambda}$ that quantifies the efficiency for the scattering light as

$$J_\lambda = \beta_{s,\lambda} F_{\odot,\lambda} e^{-\tau_\lambda/\mu_0} P_\lambda(\mu,\phi;-\mu_0,\phi_0)\frac{1}{4\pi}, \tag{2.21}$$

where $F_{\odot,\lambda}$ is the fraction of the solar flux at the TOA at this wavelength λ, $P_\lambda(\mu,\phi;-\mu_0,\phi_0)$ is the angular distribution of the scattered beam and $\frac{1}{4\pi}$ is the portion of solid angle. By definition, downward angles are taken with a minus sign.

Multiscattering processes require the consideration of the contribution of each infinitesimal element of the solid angle to the source function, i.e

$$J_\lambda = \beta_{s,\lambda}\int_0^{2\pi}\int_{-1}^{1} I_\lambda(\tau,\mu'\phi')P_\lambda(\mu,\phi;\mu',\phi')\frac{d\mu' d\phi'}{4\pi}. \tag{2.22}$$

We can define a new variable named *single scattering albedo* $\omega_{0,\lambda}$ as the ratio between the scattering (i.e. $\beta_{s,\lambda}$) and the extinction (i.e. $\beta_{ext,\lambda} = k_\lambda + \beta_{s,\lambda}$),

$$\omega_{0,\lambda} = \frac{\beta_{s,\lambda}}{\beta_{ext,\lambda}} = \frac{\beta_{s,\lambda}}{k_\lambda + \beta_{s,\lambda}}. \tag{2.23}$$

This magnitude is a very useful variable in radiative transfer. If in the case of τ_λ, we have seen that it represents the opacity of a medium, now $\omega_{0,\lambda}$ quantifies how the radiation is scattered by the medium. A medium with $\omega_{0,\lambda} = 1$ indicates that all the light is scattered

and it is called conservative case. In contrast, $\omega_{0,\lambda} = 0$ implies non-scattering, i.e. the Beer's law (Eq. 2.9).

By substituting Eqs. 2.21, 2.22 and 2.23 into Eq. 2.17, we get

$$\begin{aligned}\mu\frac{dI_\lambda}{d\tau_\lambda} = &- I_\lambda(\tau_\lambda,\mu,\phi)+ \\ &\frac{\omega_{0,\lambda}}{4\pi}\int_0^{2\pi}\int_{-1}^{1} I_\lambda(\tau_\lambda,\mu'\phi')P_\lambda(\mu,\phi;\mu',\phi')d\mu' d\phi'+ \\ &\frac{\omega_{0,\lambda}}{4\pi}F_{\odot,\lambda}e^{-\tau_\lambda/\mu_0}P_\lambda(\mu,\phi;-\mu_0,\phi_0).\end{aligned} \tag{2.24}$$

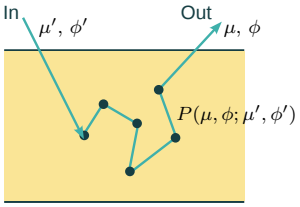

Figure 2.5: The phase function represents the angular distribution of the scattered radiation.

From Eq. 2.24, the radiative transfer problem for shortwave radiation requires to obtain an expression for τ_λ, $\omega_{0,\lambda}$ and $P_\lambda(\cos\Theta)$. As we will discuss through the following chapters, the phase function is the most difficult to determine.

Due to the mathematical properties of the Legendre polynomials, they are the best candidates to deal with the phase function. If we express $P_\lambda(\cos\Theta)$ in terms of these polynomials, we get

$$P_\lambda(\cos\Theta) = \sum_{l=0}^{N}\omega_{l,\lambda}P_l(\cos\Theta), \tag{2.25}$$

where the coefficients $\omega_{l,\lambda}$ are

$$\omega_{l,\lambda} = \frac{2l+1}{2}\int_{-1}^{1} P_\lambda(\cos\Theta)P_l(\cos\Theta)d\cos\Theta \tag{2.26}$$

with $l = 0, 1, ..., N$ and P_l is the Legendre polynomial of order l.

The first moment of the phase function (i.e. $l = 1$) can be expressed as

$$g_\lambda = \frac{\omega_1}{3} = \frac{1}{2}\int_{-1}^{1} P(\cos\Theta)d\cos\Theta, \tag{2.27}$$

This parameter is widely used and it is named *asymmetry factor*. Physically, g_λ describes how the scattered radiation is propagated through the space. In an isotropic scattering medium (e.g. Rayleigh scattering), $g_\lambda = 1$, while in a non-isotropic cases, g_λ increases as the diffraction peak becomes more significant and it can be negative if the peak is at the opposite direction of the beam propagation.

At this point, the reader may note that the dependence of all variables on λ becomes so tedious. For this reason, hereinafter we will omit this subscript with the exception of cases focused on the spectral integration.

By substituting Eq. 2.20 into Eq. 2.25, we have

$$P(\mu,\phi;\mu',\phi') = \sum_{l=0}^{N}\omega_l P_l\big(\mu\mu' + (1-\mu^2)^{1/2}(1-\mu'^2)^{1/2}\cos(\phi'-\phi)\big). \tag{2.28}$$

The mathematical properties of the Legendre polynomials (e.g. Spiegel, 1968) allow to decompose Eq. 2.28 in spherical harmonics as

$$P(\mu,\phi;\mu',\phi') = \sum_{m=0}^{N}\sum_{l=0}^{N}\omega_l^m P_l^m(\mu)P_l^m(\mu')\cos m(\phi'-\phi). \tag{2.29}$$

where

$$\omega_l^m = (2 - \delta_{0,m})\omega_l \frac{(l-m)!}{(l+m)!} \tag{2.30}$$

with $l = m, ..., N$ and $0 \leq m \leq N$. P_l^m are the associated Legendre polynomials and $\delta_{0,m}$ is the Dirac Delta function being 1 when $m = 0$ and 0 otherwise.

Similarly, the monochromatic intensity can be decomposed in spherical harmonics as

$$I(\tau, \mu, \phi) = \sum_{m=0}^{N} I^m(\tau, \mu) \cos m(\phi_0 - \phi) \tag{2.31}$$

By substituting Eqs. 2.29 and 2.31 into Eq. 2.24 and taking into account the orthogonality of the associated Legendre polynomials, we have $N + 1$ independent equations as

$$\begin{aligned} \mu \frac{dI^m(\tau, \mu)}{d\tau} =& I^m(\tau, \mu) - (1 + \delta_{0,m}) \frac{\omega_0}{4} \sum_{l=m}^{N} \omega_l^m P_l^m(\mu) \int_{-1}^{1} P_l^m(\mu') I^m(\tau, \mu') d\mu' - \\ & - \frac{\omega_0}{4\pi} \sum_{l=m}^{N} \omega_l^m P_l^m(\mu) P_l^m(-\mu_0) F_\odot e^{-\tau/\mu_0}. \end{aligned} \tag{2.32}$$

Note that we started with the general form of the RTE equation in plane-parallel atmospheres given by Eq. 2.24 and now, we have a set of $N + 1$ equations linearly independent expressed in terms of the associated Legendre polynomials. Therefore, we can solve the RTE for each I^m and then we can recover the total monochromatic intensity using Eq. 2.31.

Moreover, for most of the meteorological applications, the medium can be considered as homogeneous in the horizontal direction and thus, the dependence with the azimuth angle can be neglected. Under this approximation the phase function becomes directly,

$$P(\mu, \mu') = \sum_{l=0}^{N} \omega_l P_l(\mu) P_l(\mu'). \tag{2.33}$$

Therefore, the RTE is simplified to

$$\begin{aligned} \mu \frac{dI(\tau, \mu)}{d\tau} =& I(\tau, \mu) - \frac{\omega}{2} \int_{-1}^{1} I(\tau, \mu') P(\mu, \mu') d\mu' - \\ & - \frac{\omega}{4\pi} P(\mu, -\mu_0) F_\odot e^{-\tau/\mu_0}. \end{aligned} \tag{2.34}$$

We may assume that Eq. 2.34 has an analytic solution given by $I(\tau, \mu)$. The amount of radiation crossing one hemisphere of solid angle defines the *monochromatic flux* as

$$F^{\uparrow\downarrow} = 2\pi \int_{0}^{\pm 1} I(\tau, \mu) \mu d\mu, \tag{2.35}$$

where the upward and downward arrows indicate the upward and downward fluxes for each hemisphere defined as normal to the surface, respectively. This integration is represented by the sign +/- in Eq. 2.35.

However, Eq. 2.35 is uncompleted because the RTE has been considered in a scattering medium and consequently, this equation is only valid for solving the diffuse component of the flux, but not the single attenuation of the direct beam without scattering interactions. As a consequence, we have to include the contribution of the direct beam into the downward flux based on the Beer's law given by Eq. 2.9.

In other words, we have

$$F^{\uparrow} = 2\pi \int_0^1 I(\tau, \mu)\mu d\mu, \tag{2.36}$$

for the upward flux or *diffuse upward flux*, and

$$F^{\downarrow} = 2\pi \int_0^{-1} I(\tau, \mu)\mu d\mu + \mu_0 F_{\odot} e^{-\tau/\mu_0}, \tag{2.37}$$

for the downward flux. The first term in Eq. 2.37 is named *diffuse downward flux* or, more commonly, diffuse flux, while the second term is named *direct flux*.

Finally, the difference between both fluxes defines the *monochromatic net flux* F_λ,

$$F_\lambda = F_\lambda^{\downarrow} - F_\lambda^{\uparrow}, \tag{2.38}$$

that is always positive in the shortwave part of the electromagnetic spectrum.

Eq. 2.38 can be integrated for the entire solar spectrum (i.e. from $\lambda = \lambda_{solar,min}$ to $\lambda = \lambda_{solar,max}$ producing the net flux F,

$$F = \int_{\lambda_{solar,min}}^{\lambda_{solar,max}} F_\lambda d\lambda. \tag{2.39}$$

Due to the energy conservation principle this difference between the downward and upward fluxes must be absorbed by the atmosphere that finally is transformed into heat. The shortwave heating rate is defined as the divergence of the solar flux

$$\frac{\partial T}{\partial t} = -\frac{1}{\rho c_p}\frac{\partial F}{\partial z}, \tag{2.40}$$

where c_p is the air specific heat at constant pressure.

In NWP models, the spectral integrated fluxes at the surface and the vertical profile of the heating rate play an important role (Montornès et al., 2015e). The first one because interacts with the LSM warming the surface and producing the day-night patterns, and the second one because it contributes through the diabatic term of the energy equation to the thermal structure of the atmosphere.

The downward components of the flux are also important in solar energy applications. Generally, the interest of these fields is at the surface (i.e. vertically integrated) and they use a slightly different notation. The downward total flux is typically called global horizontal irradiance, GHI, the diffuse downward flux is called diffuse irradiance, DIF and the direct component is called direct horizontal irradiance, DHI, if it is projected with respect to the normal axis, or direct normal irradiance, DNI, if it is referred to the beam direction. The nomenclature of GHI, DHI and DIF differs slightly in some of the solar industry reports.

In this chapter, we have presented the general form of the RTE. With some general assumptions, such as the plane-parallel atmosphere approximation and horizontal homogeneity, we have reduced the complexity of the problem, providing the general form of the RTE for most of the atmospheric applications represented by Eq. 2.34. This equation is expressed in terms of three radiative variables or also called single-scattering variables: the optical thickness τ, the single scattering albedo ω_0 and the first moment of the phase function called asymmetry factor g.

At this point, we can identify some important limitations for building a solar parameterization. First, Eq. 2.34 is still complicated and it can not be transformed into an easy algorithm. In Sect. 2.3, we will discuss the most common used algorithms for solving the RTE in solar parameterizations.

The second issue is related with the vertical integration. All the discussion carried out in this chapter is valid for homogeneous mediums. However, the Earth atmosphere shows an

important non-homogeneity, mainly in the vertical fro the region represented by one grid-point. The treatment of the vertical integration will be discussed in Sect. 2.4.

Other important issues are the spectral integration and the evaluation of the radiative variables. Due to the atmospheric composition by many molecules and particles with different physical properties, the spectral integration given by Eq. 2.39 can be very complex. Moreover, the radiative variables are not a solution of the Euler equations solved by the NWP model and hence, they must be parameterized in terms of the meteorological fields available in the model (e.g. temperature, water mixing ratio or cloud droplets mixing ratio, among others). A general overview of the typical approaches for transforming the atmospheric fields to the radiative variables and performing the spectral integration will be treated in Sect. 2.5.

2.3 Approximated solution to the RTE

As aforesaid in Sect. 2.2, the computation of $F^{\downarrow}$, $F^{\uparrow}$ and heating rate requires of solving Eq. 2.32 or most specifically, Eq. 2.34. This is not an easy challenge by the wide range of values that the radiative parameters can take in the real atmosphere (Joseph et al., 1976).

Under specific conditions, Eq. 2.32 has an exact solution. In 1950, Chandrasekhar developed an elegant mathematical method named Discrete-Ordinates method (Chandrasekhar, 1950) which allowed to find a solution of the monochromatic intensity I_λ in stellar and planetary atmospheres. Lately, in 1970s and 1980s, authors such as Liou (1973) demonstrated that the method was also useful under the presence of aerosols and cloud particles. Nowadays, the method is fully detailed in many radiative transfer manuals such as in Lenoble (1993) or in Liou (2002), among others.

Basically, this method takes Eq. 2.34, and it replaces the integral in the second term of the right hand part by a finite sum of elements using the Gauss Formula (Spiegel, 1968). This approximation is a quadrature rule and it will be recurrent in other sections of this chapter. The idea is that if $f(x)$ is a *good* function (i.e. continuous and derivable), then the integral between -1 and 1 over a x domain can be substituted by a finite sum of points x_i in which the function is evaluated as

$$\int_{-1}^{1} f(x)dx \simeq \sum_{i=1}^{n} w_i f(x_i), \tag{2.41}$$

where w_i are a set of known weights.

Introducing this approximation into Eq. 2.34, the RTE becomes a first order nonhomogeneous differential equation or, in a more general way, i.e. Eq. 2.32, a set of $N+1$ equations.

This method is used in the Discrete Ordinates Radiative Transfer Program for a Multi-Layered Plane-Parallel Medium, DISORT (Stamnes et al., 1988; Stamnes, 2000), algorithm that is the core of many radiative transfer codes used in research and remote sensing applications such as Streamer (Key and Schweiger, 1998), Moderate Resolution Atmospheric Transmission, MODTRAN, (Berk et al., 1987), REST2 (Gueymard, 2008) or, Santa Barbara DISORT Atmospheric Radiative Transfer, SBDART (Ricchiazzi et al., 1998), among others.

Nevertheless, the discrete ordinate method requires a high number of computations becoming unfeasible for a NWP model parameterization. To visualize this problem, let us imagine a grid composed by 100 points in west-east and south-north directions and 51 vertical levels (i.e. 50 layers). Moreover, let us assume a radiative parameterization that divides the shortwave spectrum in 10 intervals. Therefore, if one has to solve the RTE for each spherical harmonic (i.e. $m = 0...N$) and Gauss point (i.e. $i = 1...n$), this means $100\text{x}100\text{x}50\text{x}10\text{x}(N+1)\text{x}n \sim 10^6\text{x}(N+1)\text{x}n$ computations at each radiative call, unfeasible taking in to account the typical NWP model applications (i.e. operational forecasting) and the current hardware resources.

With the goal of reducing the high usage of computational resources, the radiative transfer schemes in NWP models reduce the computation of I_λ by using approximated methods. In general, these methods are: the two-stream approximation, the Eddington approximation and the four stream approximation. All of them will be briefly presented in Sects. 2.3.1, 2.3.2 and 2.3.4, respectively.

2.3.1 Two-stream approximation

The two-stream approximation (Liou, 1973, 1974) begins as the discrete ordinate method. In virtue of the Gauss formula (Eq. 2.41), the second term in equation 2.34 is replaced by a sum of a finite number of quadrature points as

$$\int_{-1}^{1} f(\mu)d\mu \sim \sum_{j=-n}^{n} a_j f(\mu_j), \tag{2.42}$$

where the weights a_j are given by

$$a_j = \frac{1}{P'_{2n}(\mu_j)} \int_{-1}^{1} \frac{P_{2n}(\mu)}{\mu - \mu_j} d\mu, \tag{2.43}$$

μ_j are the zeros of the polynomials P_{2n}, while P'_{2n} means the derivative with respect μ. Using the Gauss formula, Eq. 2.34 can be written as

$$\mu_i \frac{dI(\tau,\mu_i)}{d\tau} = I(\tau,\mu_i) - \frac{\omega_0}{2} \sum_{l=0}^{N} \omega_l P_l(\mu_i) \sum_{j=-n}^{n} a_j P_l(\mu_j) I(\tau,\mu_j) - \frac{\omega_0}{4\pi} P(\mu,-\mu_0) F_\odot e^{-\tau/\mu_0}, \tag{2.44}$$

for $i = -n...n$.

The physical sense of the set of μ_i values with $i = -n...n$ is each one of the directions in which the beam is propagated.

Based on Eq. 2.44, the two-stream approximation assumes two beams or streams, i.e. $i = -1, 1$ and $N = 1$. Under this assumption, the following relationships apply (e.g. Liou, 2002),

$$\mu_1 = \frac{1}{\sqrt{3}}, \qquad a_1 = a_{-1} = 1, \qquad \mu_{-1} = -\mu_1. \tag{2.45}$$

Therefore, this approximation reduces the complicated analysis of the diffuse radiation to two monochromatic intensities: one representing the upper hemisphere with $I(\tau,\mu_1)$ and the other representing the lower hemisphere $I(\tau,-\mu_1)$. Hereinafter, we will write these intensities as $I^\uparrow$ and $I^\downarrow$, respectively, in order to simplify the nomenclature.

Mathematically, Eq. 2.44 splits into two first order nonhomogeneous differential equations representing each hemisphere as

$$\mu_1 \frac{dI^\uparrow}{d\tau} = I^\uparrow - \omega_0(1-b)I^\uparrow - \omega_0 b I^\downarrow - S^- e^{-\tau/\mu_0}, \tag{2.46}$$

$$\mu_1 \frac{dI^\downarrow}{d\tau} = I^\downarrow - \omega_0(1-b)I^\downarrow - \omega_0 b I^\uparrow - S^+ e^{-\tau/\mu_0}, \tag{2.47}$$

where

$$b = \frac{1-g}{2}, \qquad S^\pm = \frac{F_\odot \omega_0}{4\pi}(1 \pm 2g\mu_1\mu_0). \tag{2.48}$$

From Eqs. 2.46 and 2.47, we can note that the upward and downward intensities are interrelated as it is expected. Examining the right hand part in both expressions, we observe that the second term in Eq. 2.46 (Eq. 2.47) represents the scattering of $I^{\uparrow}$ ($I^{\downarrow}$) beam in the upper hemisphere, the third term is the scattering of $I^{\downarrow}$ ($I^{\uparrow}$) beam in the lower hemisphere and the last term is the scattering of the direct beam upward and downward.

The solution of Eqs. 2.46 and 2.47 requires two boundary conditions. In general, the diffuse radiation at the TOA and at the surface is taken as zero.

Solving this system of equations, we have

$$I^{\uparrow} = I(\tau, \mu_1) = Kve^{k\tau} + Hue^{-k\tau} + \epsilon e^{-\tau/\mu_0} \tag{2.49}$$

and

$$I^{\downarrow} = I(\tau, -\mu_1) = Kue^{k\tau} + Hve^{-k\tau} + \gamma e^{-\tau/\mu_0} \tag{2.50}$$

where

$$v = \frac{1+a}{2}, \tag{2.51}$$

$$u = \frac{1-a}{2}, \qquad a^2 = \frac{1-\omega_0}{1-\omega_0 g}, \qquad \epsilon = \frac{\alpha+\beta}{2}, \tag{2.52}$$

$$\gamma = \frac{\alpha-\beta}{2}, \qquad \alpha = \frac{Z_1\mu_0^2}{1-\mu_0^2k^2}, \qquad \beta = \frac{Z_2\mu_0^2}{1-\mu_0^2k^2}. \tag{2.53}$$

$$Z_1 = -\frac{(1-\omega_0 g)(S^- + S^+)}{\mu_1^2} + \frac{S^- - S^+}{\mu_1\mu_0} \qquad Z_2 = -\frac{(1-\omega_0)(S^- - S^+)}{\mu_1^2} + \frac{S^- + S^+}{\mu_1\mu_0}. \tag{2.54}$$

H and K are two constants determined from the boundary conditions for the diffuse intensity. Therefore, by assuming no diffuse radiation at the TOA and surface, H and K can be expressed as

$$H = -\frac{\epsilon u e^{\tau_1/\mu_0} - \gamma v e^{-k\tau_1}}{v^2e^{k\tau_1} - u^2e^{-k\tau_1}}, \qquad K = -\frac{\epsilon v e^{\tau_1/\mu_0} - \gamma u e^{-k\tau_1}}{v^2e^{k\tau_1} - u^2e^{-k\tau_1}}. \tag{2.55}$$

Further details regarding the development of these equations and the mathematical implications are presented in many manuals such as in Liou (2002).

With the assumption of no azimuth dependence, the computation of the fluxes becomes trivial as it was discussed in Eq. 2.35. Therefore, based on Eqs. 2.49 and 2.50, the diffuse fluxes are directly

$$F^{\uparrow} = 2\pi\mu_1 I^{\uparrow}, \qquad F^{\downarrow} = 2\pi\mu_1 I^{\downarrow}. \tag{2.56}$$

The set of equations presented in this section are valid in non-conservative scattering atmosphere (i.e. $\omega_0 < 1$). For conservative cases (i.e. $\omega_0 = 1$), the solution presented in

Eqs. 2.49 and 2.50 is not defined. The solution for conservative atmospheres follows a similar development and, thus, it is not included in this chapter. Moreover, for many applications, ω_0, is limited to be 0.9999, reducing the algorithm complexity.

2.3.2 Generalization of the two-stream approximation

The two-stream approximation was widely used during the 1970s and 1980s because it provided a rapid and easy form for obtaining answers to the radiative transfer problem (Meador and Weaver, 1980). As a consequence of different applications (e.g. studies related with planetary albedo of haze and clouds, irradiance in nonhomogeneous turbid atmospheres or NWP model applications), a high variety of approximations in the monochromatic intensity and in the phase function appeared. Meador and Weaver (1980) and later other authors such as Liou (2002) built a framework in which all these solutions were different approaches of the same method. In this section, we will present briefly the general form of the two-stream methodology and some of the most widely used approximations in the solar schemes analyzed in Chapter 3.

By integrating the fluxes in Eq. 2.34, we have

$$\begin{aligned}\frac{1}{2\pi}\frac{dF^{\uparrow}(\tau)}{d\tau} = &\int_0^1 I(\tau,\mu)d\mu - \frac{\omega_0}{2}\int_0^1\int_{-1}^1 I(\tau,\mu)P(\mu,\mu')d\mu' d\mu - \\ &- \frac{\omega_0}{4\pi}F_{\odot}e^{-\tau/\mu_0}\int_0^1 P(\mu,-\mu_0)d\mu,\end{aligned} \tag{2.57}$$

$$\begin{aligned}\frac{1}{2\pi}\frac{dF^{\downarrow}(\tau)}{d\tau} = &-\int_0^1 I(\tau,-\mu)d\mu + \frac{\omega_0}{2}\int_0^1\int_{-1}^1 I(\tau,\mu')P(-\mu,\mu')d\mu' d\mu + \\ &+ \frac{\omega_0}{4\pi}F_{\odot}e^{-\tau/\mu_0}\int_0^1 P(-\mu,-\mu_0)d\mu.\end{aligned} \tag{2.58}$$

These expressions may be written in a more compact form as

$$\frac{dF^{\uparrow}(\tau)}{d\tau} = \gamma_1 F^{\uparrow}(\tau) - \gamma_2 F^{\downarrow}(\tau) - \gamma_3\omega_0 F_{\odot}e^{-\tau/\mu_0}, \tag{2.59}$$

$$\frac{dF^{\downarrow}(\tau)}{d\tau} = \gamma_2 F^{\downarrow}(\tau) - \gamma_1 F^{\uparrow}(\tau) + (1-\gamma_3)\omega_0 F_{\odot}e^{-\tau/\mu_0}. \tag{2.60}$$

Both flux equations were firstly formulated by Schuster (1905) as it is detailed in Liou (2002). The coefficients γ_1, γ_2 and γ_3 depend on the set of approximations assumed in the monochromatic intensity and in the phase function.

There are several approaches in the literature (e.g. Meador and Weaver, 1980). In Table 2.1, we detail the two-stream approximations used in solar schemes presented in the next Section. For example, in the two-stream approximation detailed in the previous section, we assume two monochromatic intensities (i.e. the upward and downward) in the directions μ_1 and $-\mu_1$, while the phase function was expanded in two terms of Legendre polynomials.

Table 2.1: Coefficients in two-stream approximations used in the solar schemes

Method	γ_1	γ_2	γ_3
Two-stream	$\frac{1-\omega_0(1+g)/2}{\mu_1}$	$\frac{\omega_0(1-g)}{2\mu_1}$	$\frac{1-3g\mu_1\mu_0}{2}$
Eddington	$\frac{7-(4+3g)\omega_0}{4}$	$-\frac{1-(4-3g)\omega_0}{4}$	$\frac{2-3g\mu_0}{4}$

The Eddington approach (Eddington, 1916; Irvin, 1965; Irvine, 1975; Kawata and Irvine, 1970; Shettle and Weinman, 1970) expands the monochromatic intensity and the phase function in two terms of Legendre polynomials, i.e. $I(\tau,\mu) = I_0(\tau)+\mu I_1(\tau)$, $P(\mu,\mu') = 1+3g\mu\mu'$. Details of the mathematical development leading to the results presented in Table 2.1 are not presented in this text. Further information is presented in Shettle and Weinman (1970), Joseph et al. (1976) or Briegleb (1992).

One can find in the literature a wide number of other methods and approximations as, for example, the Hemispheric constant method (Coakley and Chylek, 1975) or the modified version of the Eddington approach (Meador and Weaver, 1980), among others. Some authors as Meador and Weaver (1980), Harshvardhan (1986) or King and Harshvardhan (1993) presented interesting reviews of all these methods.

The solution of Eqs. 2.59 and 2.60 may be expressed such as

$$F^{\uparrow} = vKe^{k\tau} + uHe^{-k\tau} + \epsilon e^{-\tau/\mu_0}, \tag{2.61}$$

$$F^{\downarrow} = uKe^{k\tau} + vHe^{-k\tau} + \gamma e^{-\tau/\mu_0}. \tag{2.62}$$

where

$$v = \frac{1}{2}\left(1 + (\gamma_1 - \gamma_2)/k\right), \tag{2.63}$$

$$u = \frac{1}{2}\left(1 - (\gamma_1 - \gamma_2)/k\right), \qquad k^2 = \gamma_1^2 - \gamma_2^2, \tag{2.64}$$

$$\epsilon = \left(\gamma_3(1/\mu_0 - \gamma_1) - \gamma_2(1-\gamma_3)\right)\mu_0^2\omega_0 F_{\odot} \qquad \gamma = -\left((1-\gamma_3)(1/\mu_0 + \gamma_1) - \gamma_2\gamma_3\right)\mu_0^2\omega_0 F_{\odot}. \tag{2.65}$$

Note that Eqs. 2.61 and 2.62 are simply a generalization of Eqs. 2.49 and 2.50 presented in the previous section.

2.3.3 δ-function adjustment

The set of methods described in the previous section are good approximations for optically thick layers with isotropic scattering. Nevertheless, these methods become inaccurate when the forward peak becomes important (Joseph et al., 1976). The main problem is that the scattering for atmospheric particles (e.g. cloud particles) has an important peak in the direction of propagation being five or six orders of magnitude higher than the backward peak.

This issue can be solved including an adjustment in the absorption and scattering. The method is detailed in many publications and manuals such as Joseph et al. (1976) or Liou (2002). Basically, the fraction of energy contained in the forward peak, denoted by f, is removed from the radiative variables τ, ω_0 and g.

Formerly, the f is related with the second moment of the phase function derived from Eq. 2.26 and it can be expressed as

$$f = \frac{\omega_2}{5}. \tag{2.66}$$

The optical thickness associated to scattering processes τ_s is adjusted as

$$\tau_s' = (1-f)\tau_s, \tag{2.67}$$

while the optical thickness associated to absorption processes, τ_a, does not need a correction because it is not affected by the forward peak, i.e.

$$\tau'_a = \tau_a. \tag{2.68}$$

The total adjusted optical thickness τ' is then,

$$\tau' = \tau'_s + \tau'_a = \tau(1 - f\omega_0), \tag{2.69}$$

being τ the total non-adjusted optical thickness.

In a similar manner, the adjusted single scattering and asymmetry factor can be written as

$$\omega' = \frac{\tau'_s}{\tau'} = \frac{(1-f)\omega}{1-f\omega}, \qquad g' = \frac{g-f}{1-f}. \tag{2.70}$$

In virtue of the *Similarity Principle for radiative transfer* (Sobolev, 1975; de Hulst, 1980; Liou, 2002), the methods detailed in the previous section can be used for determining the intensity for the adjusted atmosphere.

The incorporation of the delta-function adjustment into the two-stream approximations implied a high improvement in the accuracy of the flux computations when particles had a significant forward scattering. Joseph et al. (1976) were the first to propose the application of this method in the Eddington's approximation producing the known as δ-Eddington's approach. This approach is used in many of the parameterizations (e.g. Briegleb, 1992) that will be examined in Chapter 3.

Moreover, Zdunkowski et al. (1980) proposed a different approach in the treatment of the two-stream approximation called Practical Improved Flux Method (PIFM) with a significant improvement with respect to other investigated methods. Unfortunately, the original paper is in German and it was not available in the preparation of this work. Details regarding this method can be found in Harshvardhan (1986), Räisänen (2002) or Williams et al. (2006). The set of γ_i coefficients for these methods is presented in Table 2.2.

Notwithstanding, authors such as Harshvardhan (1986) demonstrated that the assumptions taken in Eddington and δ-Eddington's approximations lead to model the scattering in thick layers (e.g. clouds) and in a large range of μ_0 values with a high accuracy. Consequently, the δ-Eddington approach has been extensively used in many atmospheric models (Räisänen, 2002).

Table 2.2: Coefficients in two-stream approximations with delta-function adjustment used in the solar schemes

Method	γ_1	γ_2	γ_3
δ-Eddington	$\frac{7-(4+3g)\omega'_0}{4}$	$-\frac{1-(4-3g')\omega'_0}{4}$	$\frac{2-3g'\mu_0}{4}$
PIFM	$\frac{8-\omega'_0(5+3g')}{4}$	$\frac{1}{4}\left(\omega'_0(1-g')\right)$	$\frac{2-3g'\mu_0}{4}$

2.3.4 Four-stream approximation

The four-stream approximation (Liou, 1974; Liou et al., 1988) assumes two streams in upper and lower hemispheres (i.e. n=1 in Eq. 2.44), while the phase function is expanded into four terms (i.e. N=3 in Eq. 2.44).

Defining I(τ, μ_1), I(τ, μ_2), I(τ, -μ_1), I(τ, -μ_2) as I_1, I_2, I_{-1} and I_{-2}, respectively, Eq. 2.44 can be written in a matrix form as

$$\frac{d}{d\tau}\begin{bmatrix} I_2 \\ I_1 \\ I_{-1} \\ I_{-2} \end{bmatrix} = \begin{bmatrix} b_{2,-2} & b_{2,-1} & b_{2,1} & b_{2,2} \\ b_{1,-2} & b_{1,-1} & b_{1,1} & b_{1,2} \\ -b_{1,2} & -b_{1,1} & -b_{1,-1} & -b_{1,-2} \\ -b_{2,2} & -b_{2,1} & -b_{2,-1} & -b_{2,-2} \end{bmatrix} \begin{bmatrix} I_2 \\ I_1 \\ I_{-1} \\ I_{-2} \end{bmatrix} - \begin{bmatrix} b_{2,-0} \\ b_{1,-0} \\ b_{-1,0} \\ b_{-2,-0} \end{bmatrix} I_{\odot}, \tag{2.71}$$

where the terms $b_{i,j}$ with $i = \pm 1, 2$ and $j = -0, \pm 1, 2$ are given by

$$b_{i,j} = \begin{cases} c_{i,j}/\mu_i,\ i \neq j \\ (c_{i,j} - 1)/\mu_i,\ i = j. \end{cases} \tag{2.72}$$

The variables $c_{i,j}$ are

$$c_{i,j} = \frac{\omega_0}{2} a_j \sum_{l=0}^{N} \omega_l P_l(\mu_i) P_l(\mu_j),\ j = -n, ..., 0, ...n. \tag{2.73}$$

As it was discussed in the case of the two-stream approximation, the four-by-four array represents the multiscattering processes in the atmosphere, while the second term in the right hand part of Eq. 2.71 represents the scattering of the direct beam at the four directions.

Therefore, we have a system of four first order nonhomogeneous differential equations. This system can be solved assuming four boundary conditions. Analogously as the 2-stream, we assume that there is no diffuse radiation at the top and at the bottom ($\tau = \tau_1$) of the layer, i.e.

$$I_{-1,-2}(\tau = 0) = 0, \qquad I_{1,2}(\tau = \tau_1) = 0. \tag{2.74}$$

The solution of Eq. 2.71 is formerly large and it does not add new information with respect to the discussion presented in Sect. 2.3.2. For this reason, we do not include those equations in this text. They can be found in the publications cited above or in manuals such as Liou (2002).

Given the solution for I_1, I_2, I_{-1} and I_{-2}, the upward and downward fluxes at a given level τ are directly

$$F^{\uparrow}(\tau) = 2\pi(a_1\mu_1 I_1 + a_2\mu_2 I_2), \tag{2.75}$$

$$F^{\downarrow}(\tau) = 2\pi(a_1\mu_1 I_{-1} + a_2\mu_2 I_{-2}) + \mu_0 F_{\odot} e^{-\tau/\mu_0}. \tag{2.76}$$

The values μ_1, μ_2, a_1 and a_2 correspond to the regular Gauss quadrature points and weights presented in Table 2.3.

In virtue of the similarity principle of the radiative transfer (Sect. 2.3.3), we can include the delta adjustment for considering the forward peak contribution (Cuzzi et al., 1982). In that case, the method is called δ4-stream approximation.

As it was explained in Sect. 2.3.1, Eq. 2.71 is valid for non-conservative scattering atmospheres. The development for the conservative case is not detailed here because it does not add relevant information for the following discussions. More details can be found in the literature.

Table 2.3: Gauss points and weights for two-stream and four-stream approximations. Extracted from Liou (2002).

Method	n	N	$\pm\mu_n$	a_n
Two-stream	1	1	μ_1=0.5773503	a_1=1
Four-stream	2	3	μ_1=0.3399810	a_1=0.6521452
			μ_2=0.8611363	a_1=0.3478548

2.4 Vertical integration

The set of approximations discussed in the previous chapters are valid in homogeneous layers. Nevertheless, the Earth atmosphere is vertically nonhomogeneous because all the thermodynamic fields in the atmosphere show a well defined stratification producing high variations with height.

Initially, this problem can be easily solved by dividing the atmosphere into a set of layers that are chosen to be homogeneous. In this case, the RTE may be solved at each layer determining the upward and downward fluxes required for evaluating the heating rate.

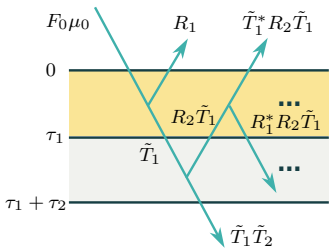

Figure 2.6: Representation of the multiscattering interaction between layers.

The main problem in this approach is that multiscattering interactions between layers with different optical properties are not considered. In order to illustrate this problem, let us assume two contiguous homogeneous layers as it is illustrated in Fig. 2.6, being τ_1 and τ_2 the optical thickness for layer 1 and 2, respectively.

When the solar beam $\mu_0 F_\odot$ reaches the first layer, one part of the radiation is upward reflected as diffuse radiation R_1, while another part is transmitted as direct and diffuse radiation $\tilde{T}_1$ into the second layer.

After crossing the first layer, $\tilde{T}_1$ interacts with the second one, experiencing an analogous process. One part of the radiation is transmitted as direct and diffuse radiation $\tilde{T}_1\tilde{T}_2$ and another part is upward reflected as diffuse radiation into the first layer $R_2\tilde{T}_1$.

Now, the first layer is illuminated from below by $R_2\tilde{T}_1$ and the process is repeated. One part of the radiation is downward reflected as diffuse radiation, $R_1^* R_2 \tilde{T}_1$ and another part is transmitted upward as $\tilde{T}_1^* R_2 \tilde{T}_1$.

Conceptually, we can repeat this process infinite times to describe the multiscattering feedback between both layers. This process can be very difficult when the atmosphere is divided in e_z layers as it occurs in a NWP model.

Therefore, we need some method for a vertical integration of the radiative fluxes. Furthermore, this method has to be efficient and should use low computational resources to be feasible in a NWP model.

The most widely used method in radiative parameterizations is the *Adding Method* (Stokes, 1862; Hansen, 1971; de Hulst, 1980) that when is coupled to the δ2-stream or δ-Eddington approximations is typically referred as δ2-stream adding method and δ-Eddington adding method, respectively.

Through the next pages, we will show a brief description of the method and its implementation in the case of e_z homogeneous layers.

2.4.1 Adding method

Let us assume a homogeneous atmospheric layer illuminated from above and from below by diffuse radiation.

If we study the layer illuminated from above (Fig. 2.7), we find that an incoming monochromatic intensity $I_{in,top}$ is reflected and transmitted as $I_{out,top}$ and $I_{out,bottom}$ described by a reflectivity R and a transmissivity $\tilde{T}$.

If we repeat this process by the layer illuminated from below (Fig. 2.7), we find that the monochromatic intensity $I_{in,bottom}$ is reflected and transmitted as $I_{out,bottom}$ and $I_{out,top}$ described by a reflectivity R^* and a transmissivity $\tilde{T}^*$.

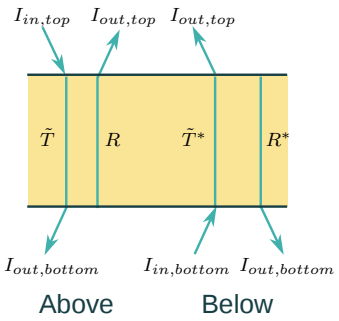

Figure 2.7: Reflectivity and transmissivity in a layer illuminated from above and below

The computation of R, R^*, $\tilde{T}$ and $\tilde{T}^*$ is directly derived from the RTE normalizing by $I_{in,top}$ and $I_{in,bottom}$ in each case.

Based on this description, let us assume two layers: 1 and 2, one on top of the other as shown in Fig. 2.8. Moreover, let us assume that R_1 and $\tilde{T}_1$ are the reflection and total transmission (i.e. direct + diffuse) at the first layer, while R_2 and $\tilde{T}_2$ are the same for the second one. Finally, let us assume that U and $\tilde{D}$ are the reflection and the transmission in the interface between 1 and 2.

We define R_{12} and $\tilde{T_{12}}$ as the combined reflectivity and transmissivity as a consequence of infinite reflections and transmissions. Following the discussion presented at the beginning of this section, we can write

$$R_{12} = R_1 + \tilde{T}_1^* R_2 \tilde{T}_1 + \tilde{T}_1^* R_2 R_1^* R_2 \tilde{T}_1 + \tilde{T}_1^* R_2 R_1^* R_2 R_1^* R_2 \tilde{T}_1 + ..., \tag{2.77}$$

$$T_{12} = \tilde{T}_2 \tilde{T}_1 + \tilde{T}_2 R_1^* R_2 \tilde{T}_1 + \tilde{T}_2 R_1^* R_2 R_1^* R_2 \tilde{T}_1 + ..., \tag{2.78}$$

$$U = R_2 \tilde{T}_1 + R_2 R_1^* R_2 \tilde{T}_1 + R_2 R_1^* R_2 R_1^* R_2 \tilde{T}_1 + ..., \tag{2.79}$$

$$\tilde{D} = \tilde{T}_1 + R_1^* R_2 \tilde{T}_1 + R_1^* R_2 R_1^* R_2 \tilde{T}_1 + ... \tag{2.80}$$

The previous series converge and they may be written as

$$R_{12} = R_1 + \tilde{T}_1^* R_2 (1 - R_1^* R_2)^{-1} \tilde{T}_1, \tag{2.81}$$

$$T_{12} = \tilde{T}_2 (1 - R_1^* R_2)^{-1} \tilde{T}_1, \tag{2.82}$$

$$U = R_2 (1 - R_1^* R_2)^{-1} \tilde{T}_1, \tag{2.83}$$

$$\tilde{D} = (1 - R_1^* R_2)^{-1} \tilde{T}_1. \tag{2.84}$$

Moreover, the following relationships will be useful for the next discussion about the method

$$S = R_1^* R_2 (1 - R_1^* R_2)^{-1}, \tag{2.85}$$

$$R_{12} = R_1 + \tilde{T}_1^* U, \tag{2.86}$$

$$T_{12} = \tilde{T}_2 \tilde{D}, \tag{2.87}$$

$$U = R_2 \tilde{D}. \tag{2.88}$$

Eq. 2.86 shows that the combined reflection due to both layers is the result of the reflection at the first layer (first term) plus the upward transmission of successive reflections between both layers (second term). On the contrary, Eq. 2.87 shows that the combined transmission is the result of the transmission through the second layer of $\tilde{D}$.

As we defined at the beginning of this explanation, the total transmissivity $\tilde{T}$ is the sum of the diffuse T and the direct beam given by the Beer's law as $e^{-\tau/\mu'}$ where $\mu' = \mu_0$ when the beam is from the Sun and $\mu' = \mu$ when the light comes directly from the μ direction.

Therefore, Eqs. 2.84 and 2.87 can be expressed as

$$\tilde{D} = D + e^{-\tau/\mu_0} = (1+S)T_1 + Se^{-\tau_1/\mu_0} + e^{-\tau_1/\mu_0}, \tag{2.89}$$

$$T_{12} = e^{-\tau_2/\mu}D + T_2 e^{-\tau_1/\mu_0} + T_2 D + \exp\big(-(\tau_1/\mu_0 + \tau_2/\mu)\big)\delta(\mu - \mu_0). \tag{2.90}$$

As it is shown in the literature (e.g. Liou, 2002), all these expressions can be written in an iterative form. When the layers are illuminated from above, R_{12} and T_{12} are determined by the following equations

$$Q = R_1^* R_2, \tag{2.91}$$

$$S = Q(1-Q)^{-1}, \tag{2.92}$$

$$D = T_1 + ST_1 + Se^{-\tau_1/\mu_0}, \tag{2.93}$$

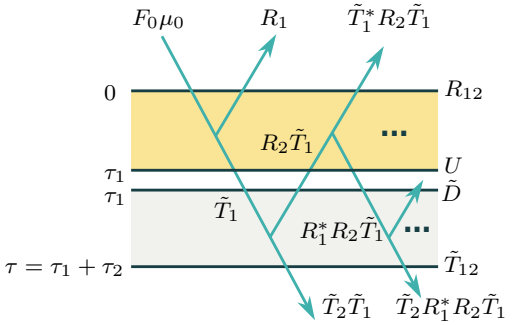

Figure 2.8: Representation of the combined combined reflectivity, R_{12}, and transmissivity, $\tilde{T_{12}}$

$$U = R_2 D + R_2 e^{-\tau_1/\mu_0}, \qquad R_{12} = R_1 + e^{\tau_1/\mu}U + T_1^* U, \tag{2.94}$$

$$T_{12} = e^{-\tau_2/\mu}D + T_2 e^{-\tau_1/\mu_0} + T_2 D. \tag{2.95}$$

And when the layers are illuminated from below, R_{12}^* and T_{12}^* may be computed as

$$Q = R_2 R_1^*, \qquad S = Q(1-Q)^{-1}, \tag{2.96}$$

$$U = T_2^* + ST_2^* + Se^{-\tau_2/\mu'}, \qquad D = R_1^* U + R_1^* e^{-\tau_2/\mu'}, \tag{2.97}$$

$$R_{12}^* = R_2^* + e^{-\tau_2/\mu}D + T_2 D, \qquad T_{12}^* = e^{-\tau_1/\mu}U + T_1^* e^{-\tau_2/\mu'} + T_2^* U. \tag{2.98}$$

From this discussion, the Adding method is shown as a useful approach to determine the fluxes at the TOA and surface. Nevertheless, the fluxes in a NWP model are needed at each layer in order to compute the heating rate.

Generally, we have e_z vertical layers that are assumed as homogeneous. Each layer is characterized by the radiative variables τ, ω_0 and g that lead to T_l, R_l, T_l^* and R_l^* for $l = 1, ..., e_z$. As the set of layers are homogeneous, we can demonstrate that $T_l = T_l^*$ and $R_l = R_l^*$.

Then, layers are added one by one downward from the TOA to compute the $R_{1,l}$ and $T_{1,l}$ for $l = 2, ..., e_z + 1$ and $R^*_{1,l}$ for $l = 2, ..., e_z$ (Fig. 2.9). This process is repeated upwards from the surface to compute R_{l+1,e_z+1} and T_{l+1,e_z+1} for $l = e_z - 1, ..., 1$.

The layer $e_z + 1$ corresponds to the surface with a reflectivity R_{e_z+1} that is computed assuming a Lambertian reflector described by the surface albedo, while the transmissivity is assumed as zero (i.e. $T_{e_z+1} = 0$).

By considering the composition of (1,l) layers, we can write

$$D = T_{1,l} + ST_{1,l} + Se^{-\tau_{1,l}/\mu_0}, \tag{2.99}$$

where $\tau_{1,l}$ is the optical thickness from the TOA to the level l, S is given by Eq. 2.96 and Q is

$$Q = R^*_{1,l} R_{l+1,e_z+1}. \tag{2.100}$$

Contrarily, the composition of (l+1,e_z+1) layers is given by

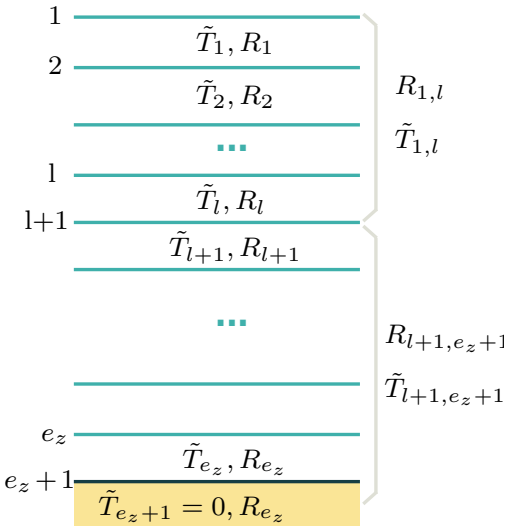

Figure 2.9: Implementation of the adding method in nonhomogeneous atmospheres

$$U = R_{l+1,e_z+1} D + R_{l+1,e_z+1} e^{-\tau_{1,l}/\mu_0}. \tag{2.101}$$

Using Eqs. 2.99 and 2.101, the flux computation at each layer becomes

$$F^{\uparrow}_{dif,l} = \mu_0 F_{\odot} \left(2 \int_0^1 U(\mu, \mu_0) \mu d\mu \right), \tag{2.102}$$

$$F^{\downarrow}_{dif,l} = \mu_0 F_{\odot} \left(2 \int_0^1 D(\mu, \mu_0) \mu d\mu \right), \tag{2.103}$$

$$F^{\downarrow}_{dir,l} = \mu_0 F_{\odot} e^{-\tau_{1,l}/\mu_0}, \tag{2.104}$$

$$F_{net,l} = (F^{\downarrow}_{dif,l} + F^{\downarrow}_{dir,l}) - F^{\uparrow}_{dif,l}. \tag{2.105}$$

2.5 Radiative variables and spectral integration

In Sect. 2.1, we have presented the general form of the RTE and its general solution in plane-parallel atmospheres, valid for stellar and planetary atmospheres. We have noted that the main problem is in the form of the source function. In Sect. 2.3, we have discussed a set of approximations for reducing the complex integro-differential form of the RTE into a set of first order differential equations. These equations are written in terms of three radiative variables, the optical thickness τ_λ, the single scattering albedo ω_0 and the asymmetry factor g. The set of approximations presented in Sect. 2.3 is only valid assuming that layers are homogeneous. However, the real atmosphere is not vertically homogeneous. For this reason, in Sect. 2.4, we have discussed the adding method, useful for performing the vertical integration of the shortwave fluxes as described by Eqs. 2.102, 2.103 and 2.104.

At this point, a further difficulty is that radiative variables are not a solution of the Euler equations and hence, they must be parameterized in terms of the i) available prognosticated

and/or diagnosed variables in the NWP model (i.e. air temperature, pressure, density, cloud droplets mixing ratio, etc) and ii) static data-sets provided by look-up tables (i.e. ozone or carbon dioxide, among others).

The form in which the physical contributions to absorption and scattering are parameterized is the core of each radiative scheme and it determines the spectral division.

In general, solar parameterizations assume different definitions for the shortwave spectrum. Typically, they start at $\sim$ 200 nm (i.e. the ultraviolet, UV), while the ending integration is more open being in the near-IR (4,000 - 5,000 nm) or even in the thermal-IR region ($\sim$ 10,000 nm). The integration over the wavelength (or wave-number) space is reduced into a few bands: from schemes that assume a single one (i.e. broadband integration) to parameterizations that use less than 20 bands. Consequently, an averaged flux $F_{\overline{\lambda}}$ is evaluated for each spectral interval and then, the total fluxes are computed as a sum over all intervals. In other words, if the solar spectrum is divided into b intervals, the total solar flux given by Eq. 2.39 is

$$F = \sum_{j=1}^{b} F_{\overline{\lambda},j} \Delta w_j, \tag{2.106}$$

where Δw_j is the fractional solar flux for the band j.

Regarding to the atmospheric gases, water vapor and ozone are the most important absorbers of solar radiation in the Earth atmosphere in cloudless and clear (i.e. without aerosols) sky conditions. These gases are parameterized with high detail. Other gases such as the molecular carbon dioxide, oxygen an nitrogen have a significant role in the absorption of solar radiation, but less important. In general, the effect of these gases are poorer represented in solar schemes. Finally, other minor gases as nitrous oxide, carbon monoxide, nitric oxide or methane exhibit an absorption spectra in the solar region (Liou, 1992) but they have a very low contribution and their effects are neglected in most of the solar parameterizations.

Originally, the absorption by the atmospheric gases was represented with parametric equations as it is shown in Stephens (1984), instead of including the effect into the RTE. Nevertheless, with the increment of the computational resources, more radiative schemes included a full description of ozone and water vapor.

The contribution of all elements (i.e. gases, clouds, aerosols) at each layer is typically composed following Cess (1985) assuming that each element is independent one to each other in the radiative transfer. Therefore, given one atmospheric layer, the total absorption optical depth τ_a is defined as the sum of the contribution of all the species as

$$\tau_a \equiv \tau_{H2O} + \tau_{O3} + \tau_{CO2} + \tau_{O2} + O(\tau), \tag{2.107}$$

where τ_{H2O}, τ_{O3}, τ_{CO2} and τ_{O2} are the optical depth of each specie and $O(\tau)$ corresponds to the contribution of the minor gases.

Given one layer bounded by heights z_1 and z_2 (with $z_1 < z_2$), the optical depth, τ_x, of each specie, x, is evaluated following Eq. 2.16 as

$$\tau_x = \int_{z_1}^{z_2} k \rho_x dz. \tag{2.108}$$

The density of the specie ρ_x can be expressed in terms of the dry air density ρ and the mixing ratio of the specie x, q_x leading to

$$\tau_x = \int_{z_1}^{z_2} k q_x \rho dz. \tag{2.109}$$

NWP models solve the Euler equations in a discretized space and time, giving the averaged state of the atmospheric fields at each grid-point, level and time-step and being unknown the sub-grid information. Therefore, a reasonable approach is to consider the absorption coefficient

as a constant within each layer. Under this assumption, Eq. 2.109 can be expressed in terms of the averaged fields as

$$\tau_x \sim k\overline{q}_x\overline{\rho}\Delta z = k\overline{u}_x, \tag{2.110}$$

where $\overline{q}_x$ and $\overline{\rho}$ are the mean values, Δz is the layer thickness and $\overline{u}_x$ is the averaged path length (Eq. 2.8). By using the hydrostatic equation, Eq. 2.110 can be easily expressed in terms of the pressure, more natural in a model that uses sigma levels or similar.

The Rayleigh scattering due to the gas molecules is evaluated in terms of the dry air content without any particularization of the gas species. In a similar manner that in the molecular absorption, we can define the optical depth due to the Rayleigh scattering, τ_s, as

$$\tau_s \sim \beta_s\overline{\rho}\Delta z, \tag{2.111}$$

where β_s is the Rayleigh scattering extinction coefficient.

Considering both scattering and absorption, the total optical depth τ of a layer is directly

$$\tau = \tau_a + \tau_s. \tag{2.112}$$

If we assume that the absorption and scattering properties remain constant in a small spectral band then, the single scattering albedo (Eq. 2.23) of the layer can be expressed as

$$\omega_0 = \frac{\tau_s}{\tau}. \tag{2.113}$$

Eqs. 2.112 and 2.113 become more complex if we introduce the absorption and scattering by aerosols and clouds particles. Both elements have an important role in the transfer of solar radiation.

If τ_{aer} and τ_{cld} are the optical thickness of aerosols and clouds then, Eq. 2.112 can be expressed as

$$\tau = \tau_a + \tau_s + \tau_{aer} + \tau_{cld} \tag{2.114}$$

and Eq. 2.113 as

$$\omega = \frac{\tau_s + \tau_{aer} + \tau_{cld}}{\tau} = \omega_s + \omega_{aer} + \omega_{cld}. \tag{2.115}$$

Each scattering process p has associated an asymmetry factor g_p. Then, the composed asymmetry factor is determined as

$$g = \frac{\sum_{i=1}^{P} g_i\omega_i\tau_i}{\sum_{i=1}^{P} \omega_i\tau_i}, \tag{2.116}$$

where P is the number of scattering contributions.

When the δ-scaling approach is used (Sect. 2.3.3), the forward peak must be also evaluated and then, Eqs. 2.69 and 2.70 can be used.

2.5.1 Atmospheric gases absorption

Absorption coefficient

The physical property that expresses the absorption efficiency of a molecule is the absorption coefficient k_λ. This coefficient depends on the atomic and electronic structure of the molecule and it is formerly expressed in terms of the line strength S and the line-shape factor $f(\lambda - \lambda_0)$ as

$$k_\lambda = Sf(\lambda - \lambda_0). \tag{2.117}$$

One molecule has three forms of internal energy: rotational, vibrational and electronic. As it is described by the quantum mechanics (Gottfried, 1993), they are defined by a set of quantum numbers. Moreover, these energies are added to the kinetic energy of the molecule that is not quantized and thus, it can exist in a range of continuum values.

The radiation absorption and emission occur when the molecule changes from one quantum state to another one. In the absorption, the molecule absorbs one photon increasing the internal energy to a higher level. In contrast, when the molecule falls from one state to another with lower energy, one photon is emitted.

The Planck's Law describes that the absorbed/emitted energy ΔE of a photon is associated with a fixed wavelength λ (or frequency) as

$$\Delta E = \frac{h}{\lambda}, \tag{2.118}$$

where h is the Planck's constant. This is called monochromatic absorption/emission.

In the atmosphere, the monochromatic absorption and emission is never observed. Due to the Heisenberg's Principle and the interaction between quantum systems, the absorption lines are broadened. Basically, there are three types of broadening: i) due to the uncertainty principle, ii) due to the pressure effect and iii) due to the Doppler effect. A full description of these processes can be found in many manuals such as Liou (2002) and for this reason they are not detailed in this chapter.

In the Earth atmosphere, the uncertainty principle can be neglected by comparison with the others. Above 20 km, there is an overlapping of the effects produced by Doppler and pressure due to the high velocity of the air molecules. Above 40 km, the Doppler broadening dominates. Nevertheless, NWP models are usually focused on the troposphere and lower stratosphere with a TOM set below 10 hPa and hence, these effects can be neglected.

Below 20 km, the pressure effects are the most important. The pressure broadening occurs by the collision between molecules. As a consequence of these collisions, molecules have associated a higher energy allowing the transition between quantum states at a different wavelengths that described by the Planck's Law.

As it is demonstrated in the literature (e.g. Liou, 2002), the line-shape factor including the pressure broadening follows the Lorentz profile and, consequently, k_λ can be written as

$$k_\lambda = \frac{S}{\pi} \frac{\alpha}{(\lambda - \lambda_0)^2 + \alpha^2}, \tag{2.119}$$

being α a scaling function defined as

$$\alpha(p, T) = \alpha_0 \left(\frac{p}{p_0}\right) \left(\frac{T_0}{T}\right)^n. \tag{2.120}$$

In Eq. 2.120, α_0 is a reference value defined at T_0 and p_0 while n is a parameter that depends on the specie. In general, the reference values are taken at 273 K and 1013 hPa used in the set of experiments and measurements in the laboratory. In virtue of Eq. 2.120, it can be demonstrated that a good approximation for k_λ is

$$k_\lambda(p, T) \cong k_\lambda(p_0, T_0) \left(\frac{p}{p_r}\right) \left(\frac{T_r}{T}\right)^n \tag{2.121}$$

This relationship is essential in the analysis and study of the radiative transfer in the Earth atmosphere (i.e. nonhomogeneous medium) because we can evaluate a single k_λ for each λ of the spectrum in the laboratory or theoretically and then, we can correct this value for a given pair of T and p values, in other words, at any height.

The approach presented in Eq. 2.121 assumes that the wavelength, temperature and pressure are decoupled. This method is called *one-parameter scaling* approximation (Howard et al.,

1956) and it is widely used in many of the solar schemes because it is simple and computationally fast (Stephens, 1984; Lacis and Oinas, 1991).

As $k_\lambda(p_0, T_0)$ does not vary with height, we can express the optical thickness in terms of a scaled path length u' as

$$\tau_\lambda = k_\lambda(p_0, T_0)u', \tag{2.122}$$

where u' is expressed as

$$u' = \int_u \left(\frac{p}{p_r}\right)\left(\frac{T_r}{T}\right)^n du. \tag{2.123}$$

The factor n has been largely discussed in the literature (e.g. Elsasser, 1960; Lacis and Hansen, 1974), concluding that the optimal value for flux and the heating rate computations is $n = 1/2$.

There are many sources of data-sets for the absorption line parameters covering a large number of spectral intervals. The most widely used in the solar parameterizations is the High-Resolution Transmission Molecular Absorption database, HITRAN, (McClatchey et al., 1973; Rothman et al., 2013). These data-sets contain information for more than 1 million lines in the range from the ultraviolet to the microwaves and including ∼50 species such as H_2O, CO_2, O_3 or O_2, among others. The absorption line is expressed in terms of four parameters: line intensity, line position, air-broadened half-width and lower-state energy, all of them defined at 296 K.

Given a set of species N and one wavelength λ, the total optical thickness τ_λ can be evaluated as the sum of the N spectral lines in λ as

$$\tau_\lambda = \sum_{j=1}^{N} \tau_{\lambda,j} = \int_u \sum_{j=1}^{N} k_{\lambda,j}(u)du. \tag{2.124}$$

This equation leads to express the absorption coefficient as

$$k_\lambda(p, T) = \sum_{j=1}^{N} S_j(T) f_{\lambda,j}(p, T). \tag{2.125}$$

Spectral integration

The only way to represent each j^{th} absorption line in Eq. 2.124 is computing k_λ at intervals smaller than the line half-width. As it is detailed in the literature (e.g. Liou, 2002), this means that k_λ must be evaluated for more than half million points. This method is called line-by-line integration (LBL) (e.g. Shulyak et al., 2004) and it is used in many high spectral resolution radiative transfer applications such as in stellar atmospheres, for instance. Although it is the most realistic method for integrating the electromagnetic spectrum, it is not feasible for most of the atmospheric modeling applications due to the high computational costs. Therefore, radiative schemes in NWP models require some simplifications in order to increase the performance.

Typically, the spectrum is divided in few bands: from one interval covering all the spectrum in called broadband spectral parameterizations to the order of tens in the most realistic schemes.

As a first order approach, we can assume the *gray atmosphere* approximation typically used in the study of stellar atmospheres. This simplification assumes that the absorption coefficient k_λ is independent of the wavelength between λ and $\lambda + d\lambda$, hence, the name of gray or without color.

Notwithstanding, this approximation is not appropriate for some atmospherics gases such as ozone, water vapor or carbon dioxide because they have a high number of spectral lines

(i.e. $\sim 10^{5-6}$) in the shortwave and longwave spectral ranges. Consequently, different approximations for considering the non-gray behavior of the Earth atmosphere are necessary.

In general, one uses a method with an acceptable accuracy that reduces significantly the number of iterations with respect to the LBL method. This approach is called *k-distribution* method (Ambarzumian and Kosirev, 1927; Arking and Grossman, 1972; Domoto, 1974; Chou and Arking, 1980). Conceptually, this method brings together the spectral transmittances, T_λ, of the gases in terms of the absorption coefficient k_λ.

As it is shown in Lacis and Oinas (1991), the spectral transmittance in homogeneous atmosphere is independent of how the k values are ordered in a given spectral interval $\Delta\lambda$. In this case, the integration in the space of λ can be substituted by an integration in the space of k. In other words,

$$T_\lambda(u) = \int_{\Delta\lambda} e^{-k_\lambda u} \frac{d\lambda}{\Delta\lambda} = \int_0^\infty e^{-ku} f(k) dk, \tag{2.126}$$

where $f(k)$ is the normalized probability distribution for k_λ at the interval $\Delta\lambda$.

We can note that the function $f(k)$ in Eq. 2.126 is just the inverse of the Laplace transformation of the spectral transmittance,

$$f(k) = \mathscr{L}^{-1}\left(T_\lambda(u)\right). \tag{2.127}$$

Additionally, we can define the cumulative probability function as

$$g(k) = \int_0^k f(k) dk. \tag{2.128}$$

In virtue of the Gauss formula (Eq. 2.41), we can rewrite Eq. 2.126 as

$$T_\lambda(u) = \int_0^1 e^{-k(g)u} dg \sim \sum_{j=1}^{M} e^{-k(g_j)u} \Delta g_j, \tag{2.129}$$

Therefore, the spectral integration between λ and $\lambda + d\lambda$ can be simplified as a finite sum of elements expressed in terms of the $k(g_j)$ and g_j data-sets that can be evaluated previously and saved in look-up tables.

Once the monochromatic flux computations are carried out for all the sub-spectral intervals, the solar flux for a spectral interval $\Delta\lambda$ can be computed as the sum of all the M intervals as

$$F_{\overline{\lambda}} = \int_{\Delta\lambda} F_\lambda \frac{d\lambda}{\Delta\lambda} = \sum_{j=1}^{M} F_j \Delta g_j \tag{2.130}$$

The variant of the k-distribution method for nonhomogenous atmospheres is the *Correlated K-distribution* method (CKD), firstly proposed by Lacis and Oinas (1991) and later developed by other authors as Fu and Liou (1992) or Kato and Ackerman (1999), among others.

Based on the definition of the optical thickness presented in Eq. 2.15, we can express the optical thickness in a nonhomogenous optical length as

$$\tau_\lambda = \int_0^u k_\lambda du = \sum_i k_{\lambda,i} \Delta u_i. \tag{2.131}$$

From this equation, the spectral transmittance can be expressed as

$$T_{\overline{\lambda}}(u) = \int_{\Delta\lambda} e^{-\tau_\lambda} d\lambda = \int_o^\infty e^{-k^* u} f(k^*) dk^*, \tag{2.132}$$

where

$$k^* = \frac{\tau}{u} = \sum_i k_i a_i, \tag{2.133}$$

$$a_i = \frac{\Delta u_i}{u} \tag{2.134}$$

and $f(k^*)$ is the probability density function of k^*. As in the case of the k-distribution method, we can define the cumulative associated probability function $g^*(k^*)$ as

$$g^*(k^*) = \int_0^{k^*} f(k^{*'}) dk^{*'} \tag{2.135}$$

Now, g^* is a function of the pressure and temperature along the nonhomogeneous path. Therefore, the spectral transmittance in $\Delta\lambda$ is

$$T_{\overline{\lambda}}(u) = \int_0^1 \exp\left(-u \sum_i k_i(g) a_i\right) dg^* \tag{2.136}$$

Assuming that g^* is independent of the pressure and temperature, Eq. 2.136 can be approximated to

$$T_{\overline{\lambda}}(u) \sim \int_0^1 \exp\left(-u \sum_i k_i(g) a_i\right) dg \tag{2.137}$$

Formerly, this means that g is correlated throughout the atmosphere and is not a function of the pressure and temperature. For this reason, Eq. 2.137 is called correlated k-distribution method.

Ozone

This gas is found in two atmospheric regions with a different impact on the radiative transfer (WMO, 2010). Most ozone ($\sim$90%) is located in the stratosphere. A layer with the highest ozone concentration that is typically found between 10 and 50 km above the surface is often referred as the ozone layer. The remaining ozone ($\sim$10%) is found in the troposphere. The highest values in this layer are located near the surface and they are mainly related to human activities.

The absorption by ozone in the solar spectral region occurs in three spectral bands (Inn and Tanaka, 1953; Anderson and Mauersberger, 1992): Hartley, Huggins and Chappuis. The Hartley bands are the strongest covering the ultraviolet (UV) from 200 to 300 nm. This absorption of solar flux is located primarily in the upper stratosphere and in the mesosphere. The other two bands are weaker. The Huggins bands operate in a UV region from 300 to 360 nm. Energy absorption in this spectral range occurs in the lower stratosphere and in the troposphere. Finally, the Chappius bands cover the photosynthetic active region (PAR) and the near-IR from 400 to 850 nm. The absorption by the Chappius bands is mainly located in the troposphere.

The absorption of the solar flux by ozone produces a heating rate ranging from 10 to 30 K day^{-1} in the stratosphere. This absorbed energy is an important physical process in maintaining the stratospheric thermal structure (Ramanathan and Dickinson, 1979).

NWP models, in general, and mesoscale NWP models, in particular, do not consider prognostic or diagnostic equations for ozone and its photochemical processes. In order to reduce the computational resources, the shortwave schemes in mesoscale NWP models simplify the ozone information. These simplifications include zonal averages and latitudinal, vertical and seasonal discretization that vary between shortwave parameterizations (Montornès et al.,

2015d). However, as it is detailed in Montornès et al. (2015e), the ozone profile has an important role for maintaining the thermal structure of the stratosphere during the simulation.

The absorption coefficient of ozone varies by several orders of magnitude in the UV and PAR regions but smoothly with the wavelength (Chou and Suarez, 1999). Consequently, many schemes assume the gray atmosphere approximation in the treatment of the ozone absorption, i.e. assuming a constant $k_{\lambda,O3}$ for each band interval. Moreover, as the absorption coefficient of ozone shows a low variation with pressure and temperature, there are schemes that neglect the scaling factor presented in Eq. 2.122.

Following Eq. 2.110, the optical thickness for a layer is generally evaluated as

$$\tau_{O3} \sim k_{O3}\overline{q}_{O3}\overline{\rho}\Delta z = k_{O3}\overline{u}_{O3} = k_{O3}\overline{q}_{O3}\overline{u}_{dry}. \tag{2.138}$$

Water vapor

Water vapor is particularly abundant in the troposphere and it shows a high variation in space and time. This gas is mostly produced by evaporation or sublimation at surface and transported through the atmosphere by different processes such as turbulent mixing, convection and cloud microphysics. Concurrently, water vapor is removed from the atmosphere by condensation (e.g. cloud droplets), freezing (e.g. ice crystals) and precipitation.

With CO_2 and CH_4, water vapor plays an important role in the greenhouse effect that produce the appropriate conditions for life in Earth.

Since this gas is the main element of solar heating in the troposphere and due to its importance for life and human activities, water vapor is included in the Euler equations solved by NWP models and it is an input for most of the physical parameterizations such as the LSM, the microphysics or the radiative transfer (Montornès et al., 2015e).

In the solar spectrum, water vapor absorption lines cover the near-IR (i.e. from 700 nm to 4.000 nm). The form of the water vapor molecule leads to a more complex treatment of the absorption than in the case of ozone. As it is indicated by Lacis and Hansen (1974) this difficulty arises from three factors. First because k_λ for water vapor is high wavelength-dependent. Second because of absorption and scattering can appear in the same region of the atmosphere. Finally, because the k_λ shows a high dependence on pressure.

Typically, we found two different approaches to the problem. Some schemes incorporate the contribution of the water absorption by using different parameterizations or empirical relationships such as the proposed by Lacis and Hansen (1974) or Liou and Sasamori (1975), among others. This kind of approaches were interesting when the computational costs were too expensive to be assumed by the operational models.

The other approach consists into incorporating the water vapor in the RTE computation. As k_λ varies rapidly with the wavelength, the CKD method is the most suitable approach. Therefore, following Eq. 2.137, each spectral band is divided into a set of pseudo-bands or g-point values.

The computation at each layer is defined in terms of the water vapor path u_{H2O}. Given one layer Δz, the optical length for water vapor u_{H2O} is evaluated as

$$u_{H2O} = \overline{q}_{H2O}\overline{\rho}\Delta z = \overline{q}_{H2O}\overline{u}_{dry}. \tag{2.139}$$

Minor gases

Generally, solar schemes have different sensibilities against the minor gasses. Some schemes neglect their contribution and the others consider them with a lower detail than in the case of ozone and water vapor.

Between all the minor gases, two are specially considered in most of the solar schemes: CO_2 and O_2. Carbon dioxide shows several spectral bands in the solar region but most of

them are so weak (e.g. 2,000 or 4,300 nm, among others) and for practical purposes can be neglected (Liou, 1992). The band at 2,700 nm, that it is overlapped with water vapor, exhibits a higher contribution to solar absorption in the lower stratosphere and it is considered explicitly in some schemes. The concentration of this gas is typically considered as a constant with height, coordinates and time.

The treatment of oxygen is easier to handle than CO_2 because the absorption occurs in a narrow spectral region free of other absorbers. In general, solar schemes assume simple approximations for this gas with a concentration of about 23%.

The features of the other minor gasses are not discussed in this text and further details can be found in the literature (e.g. Chou and Suarez, 1999 or Liou, 2002).

As the set of approaches for considering the contribution of these gases varies from one scheme to the other. They will be discussed in the analysis of the different schemes presented in Chapter 3.

2.5.2 Atmospheric gases scattering: Rayleigh

Typically, the effects of the molecular scattering are not considered explicitly for each gas species and they are simplified assuming directly the dry air mass resulting of the integration of the Euler equations. Therefore, the scattering variables (i.e. ω_0 and g) for the different species are not considered. In contrast, two variables $\omega_{0,R}$ and g_R are defined representing the scattering of the air. The single scattering albedo and asymmetry factor are set to 1 (i.e. conservative case).

The extinction optical thickness τ_R is defined in terms of the averaged density of the layer $\overline{\rho}$, the layer thickness Δz and a coefficient extinction k_R as

$$\tau_R = \beta_R \overline{u}_{dry} = \beta_R \overline{\rho} \Delta z. \tag{2.140}$$

Usually, solar schemes assume the gray atmosphere approximation considering β_R as a constant at each spectral band.

2.5.3 Aerosols

Aerosols are small particles related with many processes in the Earth atmosphere interacting directly or indirectly with the radiation budget and climate. As direct effects, aerosols increase the light scattering and opacity. By contrast, the indirect effect aerosols are involved in cloud microphysics producing changes in clouds composition.

Despite of the interest of aerosols in the atmosphere, historically, operational mesoscale models have not treated this issue in detail. On the one hand, due to the high complexity for determining their spatial distribution, vertical profile and chemical properties. On the other hand, because for an accurate fit, it is necessary a chemical package coupled to the meteorological model.

For the radiative transfer studies, the direct effects of aerosols are the most relevant. Contrary to air molecules, the common size of the aerosol particles lead to produce Mie scattering. The solution of Mie scattering for spherical particles can be exactly determined. However, this is not useful in solar schemes due to the elevated computational costs.

Instead of this, the radiative properties of the aerosols are summarized by integrated quantities: the extinction coefficient, scattering efficiency, single scattering albedo and asymmetry factor. These values are pre-computed for each species and wavelengths.

As NWP models do not solve prognostic or diagnostic equations for aerosols, many of the solar parameterizations include background climate profiles with more or less complexity.

While for most of the weather (not climate) simulations, aerosols can be neglected, the growth of the solar energy has increased the interest for improving these data-sets during the last years (e.g. Ruiz-Arias et al., 2012; Jimenez et al., 2015).

2.5.4 Clouds

Clouds are the atmospheric elements with the highest contribution in the radiative transfer. They absorb, reflect and transmit solar radiation.

The optical thickness is the most important radiative variable in the description of the optical properties of clouds (Stephens, 1978a). In the Earth atmosphere, we can find a high variety of clouds (e.g. cumulonimbus, cirrus, etc) with large differences in the composition that produce a wide range of values in τ_{cld} from 5 to 500. In general, the solar disk is hidden by clouds (i.e. the direct component of the flux, $F^{\downarrow}_{dir}$ becomes zero) when $\tau_{cld} \leq$10 as discussed in Twomey (1976).

Clouds are composed by different species of hydrometeors (e.g. water droplets, ice crystals, rain droplets, etc) that in practice can be assumed as particles that absorb and scatter light. Most of the solar schemes reduce these hydrometeors in to two classes: water droplets and ice crystals. In some cases, the other hydrometeors are aggregated to these groups introducing small corrections.

The need for a different treatment in cloud water droplets and cloud ice crystals is because the extinction coefficient for ice clouds is lower than for water clouds. On the one hand, ice crystals are bigger than water droplets and, on the other hand, the refraction indeces for both particles are significantly different (e.g. Collins et al., 2004).

In terms of the radiative transfer, the optical properties of clouds required for radiative schemes in NWP models are β_{ext}, ω_0 and g. Assuming that cloud particles are spheres, these properties can be derived from the Mie's Theory (e.g. Hulst, 1957) and from the refraction index of water (e.g. Palmer and Williams, 1974).

The extinction and scattering coefficients, β_{ext} and β_{sca}, are formerly defined as

$$\beta_{ext} = \frac{\pi}{k^3} \int_0^\infty n(r) r^2 Q_{ext}(r,k) dr \tag{2.141}$$

$$\beta_{sca} = \frac{\pi}{k^3} \int_0^\infty n(r) r^2 Q_{sca}(r,k) dr \tag{2.142}$$

being r the radius of the droplet, $k = 2\pi/\lambda$, $n(r)$ the size droplet distribution and Q_{ext} and Q_{sca}, two efficiency factors for extinction and scattering, respectively.

From Eq. 2.141, the optical thickness of a cloud can be expressed as

$$\tau_{cld} = \int_0^{\Delta z} \int_0^\infty n(r) Q_{ext}(r,k) \pi r^2 dr dz, \tag{2.143}$$

being Δz is the cloud thickness.

Slingo and Schrecker (1982) demonstrated a small variation of Q_{ext} with k, overall when k is high, tending to a asymptotic value near to 2,

$$\lim_{k \to \infty} Q_{ext} \sim 2. \tag{2.144}$$

Therefore, for small wavelengths, as in the case of the solar radiation, τ_{cld} can be approximated as

$$\tau_{cld} = \int_0^{\Delta z} 2\pi \left(\int_0^\infty n(r) r^2 dr \right) dz. \tag{2.145}$$

In practice, the integral over all the hydrometeors sizes in a cloud presented in Eq. 2.145 is useless because this information is not produced by a NWP model. Hansen and Travis (1974) proposed an effective radius as the ratio between the total volume and the cross section area,

$$r_e = \frac{\int_0^\infty n(r) r^3 dr}{\int_0^\infty n(r) r^2 dr}, \tag{2.146}$$

that simplifies this problem.

By inserting Eq. 2.146 into Eq. 2.145, the optical thickness for one type of hydrometeor h, $\tau_{cld,h}$ becomes simply

$$\tau_{cld,h} = \frac{3}{2}\frac{W_h}{r_{e,h}}, \tag{2.147}$$

where W_h is the content of the hydrometeor h in Δz.

Typically, radiative codes assume that clouds are uniform with respect to the distribution of sizes (Stephens, 1978a). In this case, W_h is directly

$$W_h = w_h \Delta z = \overline{q}_h \overline{\rho} \Delta z = \overline{q}_h \overline{u}_{dry}. \tag{2.148}$$

For water clouds W_h is called *liquid water content* (LWC) while for ice clouds W_h is named *ice water content* (IWC).

The physical sense of the variable r_e is slightly different for cloud droplets and for ice crystal. In the first case, we assume spherical particles with an effective radius $r_{e,w}$ given by

$$r_{e,w} = \frac{3}{4\rho_w}\frac{C}{A_c}, \tag{2.149}$$

where ρ_w is the water density, A_c is the effective cloud fraction and C is the cloud mass concentration per unit of volume.

Instead, ice crystals are assumed as hexagonal and randomly oriented in the space. In this case, r_e is called effective size $r_{e,i}$ defined as

$$r_{e,i} = \frac{2\sqrt{3}}{3\rho_i}\frac{C}{A_c}, \tag{2.150}$$

with ρ_i, the ice density.

The discussion for $\omega_{0,cld}$ and g_{cld} becomes more complicated and, consequently, there are several approximations as detailed in Chou and Suarez (1999). Physically, the single scattering albedo for cloud particles varies several orders of magnitude within the shortwave spectrum. Thus, it is extremely difficult to find an effective single scattering albedo for broad spectral bands that can be used in situations of strong and weak absorption.

Furthermore, the solar absorption by clouds is a function of the water vapor amount and the phase of the particles (i.e. liquid or ice). Consequently, there is not an optimal way for evaluating the ω_0 in a broad spectral interval.

In contrast to ω_0 and g, β_s varies smoothly with the wavelength. As it is detailed in Chou and Suarez (1999), theoretical works such as Tsay et al. (1989), Hu and Stamnes (1993) or Fu (1996), among others have demonstrated that the radiative variables for clouds are not significantly affected by factors as the particle size distribution and thus, they can be parameterized in terms of the effective radius/size described above.

Typically, it is used the approach presented by Slingo and Schrecker (1982), or with small variations, in which the radiative variables are defined as

$$\beta_s = a_{0,s} + \frac{a_{1,s}}{r_{e,s}}, \tag{2.151}$$

$$1 - \omega_{0,s} = b_{0,s} + b_{1,s} r_{e,s} + b_{2,s} r_{e,s}^2, \tag{2.152}$$

$$g_s = c_{0,s} + c_{1,s} r_{e,s} + c_{2,s} r_{e,s}^2, \tag{2.153}$$

where $a_{i,s}$, $b_{i,s}$ and $c_{i,s}$ are the regression coefficients that fit empirical data-sets and the subscript s indicates that they are different for each cloud particle specie (i.e. cloud droplets, ice crystals). The idea for ice crystals is similar as it is shown in Liou et al. (2008).

Using Eq. 2.151, the optical thickness τ_s in a layer Δz is directly

$$\tau_s = \beta_s q_s \rho \Delta z \tag{2.154}$$

Although, the radiative variables can be determined in a more or less easy way, the addition of clouds into the radiative computations presents important problems. In the atmosphere, clouds are located at different heights with different sky covering and optical properties. Nevertheless, the set of approximations presented in Sects. 2.2 and 2.3 assume the plane-parallel approach, hence, the horizontal nonhomogeneity is not allowed.

For illustrating this problem, suppose a domain R of tens or hundreds of kilometers with a 3-dimension distribution of the cloud properties known exactly as proposed in Pincus et al. (2003). In this domain, the averaged and spectral integrated flux $< F >$ can be written as

$$< F >= \frac{1}{\Delta x \Delta y \Delta z} \int S(\lambda) \left(\int \int \int_R F_{3D}(x, y, z, \lambda) dz dx dy \right) d\lambda, \tag{2.155}$$

where $S(\lambda)$ is the portion of energy at $d\lambda$ and $F_{3D}(x, y, z, \lambda)$ is the analytic form of the monochromatic flux. Δx, Δy and Δz are the domain dimensions.

For the characteristic scales occurring in the synoptic scale and mesoscale the horizontal variations of the flux can be considered as negligible and therefore, we can assume atmospheric columns as independent one to each other. This is called independent column approximation (ICA). Under this approximation, the vertical integration in Eq. 2.155 can be performed with the methods discussed in the previous sections. Therefore, we can write $< F^{ICA} >$ such as

$$< F^{ICA} >= \frac{1}{\Delta x \Delta y} \int S(\lambda) \left(\int \int_R F_{2D}(x, y, \lambda) dx dy \right) d\lambda, \tag{2.156}$$

The main problem in this approach is that fluxes are more horizontally homogeneous in clear sky scenarios than in cloudy ones due to the texture of clouds that can show complex spatial distributions. The most commonly used approximation for solving this issue is to consider the clear sky flux $< F_{clr}^{ICA} >$ and the cloudy sky flux $< F_{cld}^{ICA} >$ separately, i.e.

$$< F^{ICA} >= (1 - C) < F_{clr}^{ICA} > + C < F_{cld}^{ICA} >, \tag{2.157}$$

being C the cloud cover.

One typical approach in the treatment of the partial cloud coverage is dividing each layer in sections. At each section, the atmosphere is assumed as fully cloudless or overcasted by a homogeneous cloud. Then, the radiative fluxes are evaluated at each region and the results are summed weighting with the cloud fraction. In other words, we can express Eq. 2.156 as an integral over the distribution $p(s)$ of all possible cloudy configurations s,

$$< F^{ICA} >= (1 - C) \int S(\lambda) F(\lambda) d\lambda + C \int S(\lambda) \left(\int p(s) F(s, \lambda) ds \right) d\lambda, \tag{2.158}$$

In a NWP model, the ICA can be applied naturally over each grid-point producing the averaged flux at each node.

The main problem in this method is that depending on the number of layers with clouds and the manner in which these clouds are overlapped, the computational costs can increase considerably because these steps must be performed for each spectral band

There are many strategies for reducing the number of computations. In the next sections, we will discuss the most widely used in the solar schemes analyzed in Chapter 3: Maximum-random cloud overlapping and Monte Carlo Independent Column, MICA (Pincus et al., 2003).

Maximum-random cloud overlapping

The maximum cloud overlapping is a particular case of the available techniques for considering the cloud overlap (Morcrette and Fouquart, 1986): random, minimum, maximum or a linear combination of layer transmissivities and reflectivities. Typically, the most widely used methods are the random overlapping, the maximum overlapping or an hybrid of both.

However, as it is suggested by some authors such as Morcrette and Fouquart (1986), the selection of one approach or another should be linked with the spatial scale resolved by the model. In the same paper, the author provides some examples that illustrates the problem. For example, in a model with a coarse resolution, one grid cell of 10x10 km may represent a cumulus cloud in one corner and a cirrus located in the opposite corner without overlap. In that case, the minimum overlapping method should be the most appropriated approach.

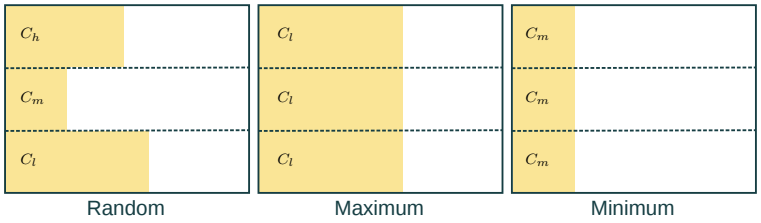

Figure 2.10: Conceptual idea of the techniques for considering the cloud overlapping (Morcrette and Fouquart, 1986).

In order to figure out the differences between these methods, let us assume three layers with clouds: low, mid and high with the respective cloud covers C_l, C_m and C_h.

In the random overlap method, layers with clouds are considered as independent (Fig. 2.10). In that case, we can define eight combined cloud covers representing different cloud distributions. The combined clear sky fraction C_{clr} is easily

$$C_{clr} = (1 - C_l)(1 - C_m)(1 - C_h) = \prod_{i=1}^{3}(1 - C_i). \tag{2.159}$$

We can consider three combined fractions, C_j^1, in which only one layer is covered by clouds

$$C_j^1 = C_j \prod_{i \neq j}^{i=1,2,3} (1 - C_i), \tag{2.160}$$

three combined fractions, C_j^2, in which two layers are overlapped

$$C_j^2 = C_i C_j (1 - C_k), \tag{2.161}$$

and one combined fraction with all layers overlapped, C^3,

$$C^3 = C_i C_j C_k, \tag{2.162}$$

where i,j,k represent each layer.

In a similar manner, we can define four combined cloud fractions in the maximum overlap case as

$$C_{clr} = 1 - \max(C_l, C_m, C_h), \tag{2.163}$$
$$C_j^1 = \max(0, C_j - \max(C_i, C_k)), \tag{2.164}$$
$$C_j^2 = \max(0, \min(C_i, C_j) - C^3)), \tag{2.165}$$
$$C^3 = \min(C_l, C_m, C_h). \tag{2.166}$$

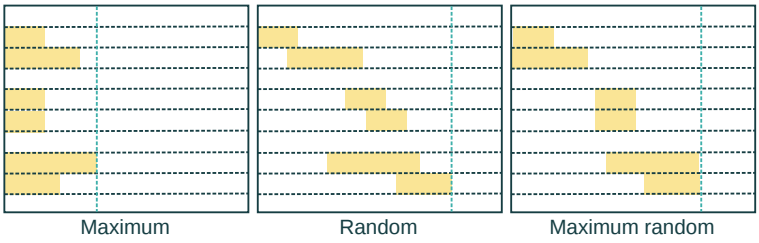

Figure 2.11: Conceptual idea of the maximum random overlap based on Morcrette and Fouquart (1986).

The random case implies the computation of the RTE for eight different scenarios while the maximum case the RTE has to be evaluated for four scenarios. Logically, this approach increases significantly the computational time. Finally, the composed flux is evaluated as a linear combination of these configurations weighted by the fractions C_{clr}, C_j^1, C_j^2 and C^3 as

$$F_\lambda = \sum_{j=1}^{N} C_j F_{j,\lambda}. \tag{2.167}$$

The assumption of all the cloud layers in a column of a grid cell overlapped is in many cases an exaggeration, overall in a mesoscale simulation. This problem is solved with an hybrid approach called maximum random overlap. In this strategy, clouds layers are clustered in three groups: low, mid and high with boundaries often set to 700 and 400 hPa. Then, clouds in adjacent layers are considered as maximally overlapped while the groups of clouds are assumed as randomly overlapped (Fig. 2.11).

Monte Carlo Independent Column Approximation (MCICA)

The term containing the cloud contribution in Eq. 2.158 includes a two dimensional integration: on the one hand, we have the integration over the wavelength, and on the other hand, we have the integration over all the cloud configurations.

One way to reduce the computational costs is substituting the contribution of each configuration at each λ by a set of random configurations for each interval spectra as

$$< F_{cld}^{ICA} > \sim \sum_{k=1}^{K} w(\lambda_k) S(\lambda_k) F(s_{random}, \lambda_k). \tag{2.168}$$

This means that the flux at each spectral interval is evaluated as a random configuration based on the probability distribution $p(s)$ of all the possible configurations in a column. This description is just the Monte Carlo method in statistics. For this reason, this method in called Monte Carlo Independent Column Approximation.

As discussed in Pincus et al. (2003), this approximation introduces a sampling error when K is small. However, this is a random error and, for $K \to \infty$, it reaches a near 0 averaged bias.